Phonon Thermal Hall Effect in Strontium Titanate

Xiaokang Li,[1,2] Benoît Fauqué,[3] Zengwei Zhu,[2] and Kamran Behnia[1,4]
[1]Laboratoire de Physique et d'Etude des Matériaux (CNRS) ESPCI Paris, PSL Research University, 75005 Paris, France
[2]Wuhan National High Magnetic Field Center and School of Physics, Huazhong University of Science and Technology, Wuhan 430074, China
[3]JEIP, USR 3573 CNRS, Collège de France, PSL University, 11, place Marcelin Berthelot, 75231 Paris Cedex 05, France
[4]II. Physikalisches Institut, Universität zu Köln, 50937 Köln, Germany

(Received 16 September 2019; accepted 20 February 2020; published 9 March 2020)

It has been known for more than a decade that phonons can produce an off-diagonal thermal conductivity in the presence of a magnetic field. Recent studies of thermal Hall conductivity, κ_{xy}, in a variety of contexts, however, have assumed a negligibly small phonon contribution. We present a study of κ_{xy} in quantum paraelectric $SrTiO_3$, which is a nonmagnetic insulator and find that its peak value exceeds what has been reported in any other insulator, including those in which the signal has been qualified as "giant." Remarkably, $\kappa_{xy}(T)$ and $\kappa(T)$ peak at the same temperature and the former decreases faster than the latter at both sides of the peak. Interestingly, in the case of La_2CuO_4 and α-$RuCl_3$, $\kappa_{xy}(T)$ and $\kappa(T)$ peak also at the same temperature. We also studied $KTaO_3$ and found a small signal, indicating that a sizable $\kappa_{xy}(T)$ is not a generic feature of quantum paraelectrics. Combined to other observations, this points to a crucial role played by antiferrodistortive domains in generating κ_{xy} of this solid.

DOI: 10.1103/PhysRevLett.124.105901

In most insulators, thermal conductivity can be understood with reasonable accuracy by picturing phonons as carriers of heat scattered either by other phonons or by defects and boundaries [1]. An impressive agreement between experimental data near room temperature and *ab initio* solutions of the Peierls-Boltzmann equation has been achieved in the last few years [2]. Since phonons are neutral quasiparticles lacking magnetic moment, one may assume that their path is not affected by a magnetic field and therefore, in contrast to magnons and electrons, they cannot give rise to a transverse response. However, experiments carried out more than a decade ago [3] showed that there is a finite measurable phonon Hall effect. The appearance of a finite transverse thermal gradient upon application of a longitudinal heat current, implied a finite κ_{xy} in $Tb_3Ga_3O_{12}$, a paramagnetic insulator [3,4]. The experimental observation motivated numerous theoretical studies [5–11] invoking a variety of possible sources of phonon Hall effect including spin-phonon coupling [5–7], phonon Berry curvature [8,9], skew scattering [10] or simply ionic bonding [11].

During the past few years, thermal Hall effect was studied in magnetic insulators [12–14], spin-liquid candidates [15,16] and multiferroics [17]. These studies of κ_{xy} mostly assumed a marginal contribution by phonons and the detected signal was often (but not always [16]) attributed to magnetic excitations. More recently, κ_{xy} has been measured in the Kitaev spin-liquid candidate α-$RuCl_3$ [18–20] and in cuprates [21]. In both cases, the observed signal was assumed to exceed significantly what could be purely a phononic contribution.

In this Letter, we present a study of thermal Hall effect in $SrTiO_3$ crystals, a quantum paraelectric [22] with a variety of remarkable properties [23]. We found a sizable κ_{xy} in this solid. Since phonons are the unique heat carriers in this nonmagnetic band insulator, it is hard to see how carriers other than phonons can cause the observed κ_{xy}. The magnitude of the observed signal is twice larger than what was reported in $LaCuO_4$ [21]. However, at 15 T, κ_{xy} remains 400 times smaller than κ_{xx} and calling this a "giant" thermal Hall effect [17,21] does not appear as an illuminating choice.

The study of three different crystals showed that while the peak κ_{xy} can vary from one sample to another, the overall temperature dependence remains the same. This sample dependence is reminiscent of what was reported in α-$RuCl_3$ [18–20]. Comparing the temperature dependence of κ and κ_{xy} in $SrTiO_3$, it becomes clear that they both peak at the same temperature, but the decrease in κ_{xy} is sharper both below and above the peak temperature. We note that in both α-$RuCl_3$ [20] and La_2CuO_4 [21] κ and κ_{xy} peak at the same temperature. We also studied $KTaO_3$, another quantum paraelectric with no antiferrodistortive (AFD) transition and found that its κ_{xy} is much smaller. This observation indicates a crucial role played by polar domain walls of $SrTiO_3$ in generating κ_{xy}. This hypothesis is strengthened by detailed study of how the amplitude of the signal in the same sample is affected by its thermal history after trips across the 105 K structural transition.

A member of the perovskite ABO_3 family, $SrTiO_3$ avoids a ferroelectric instability thanks to the quantum

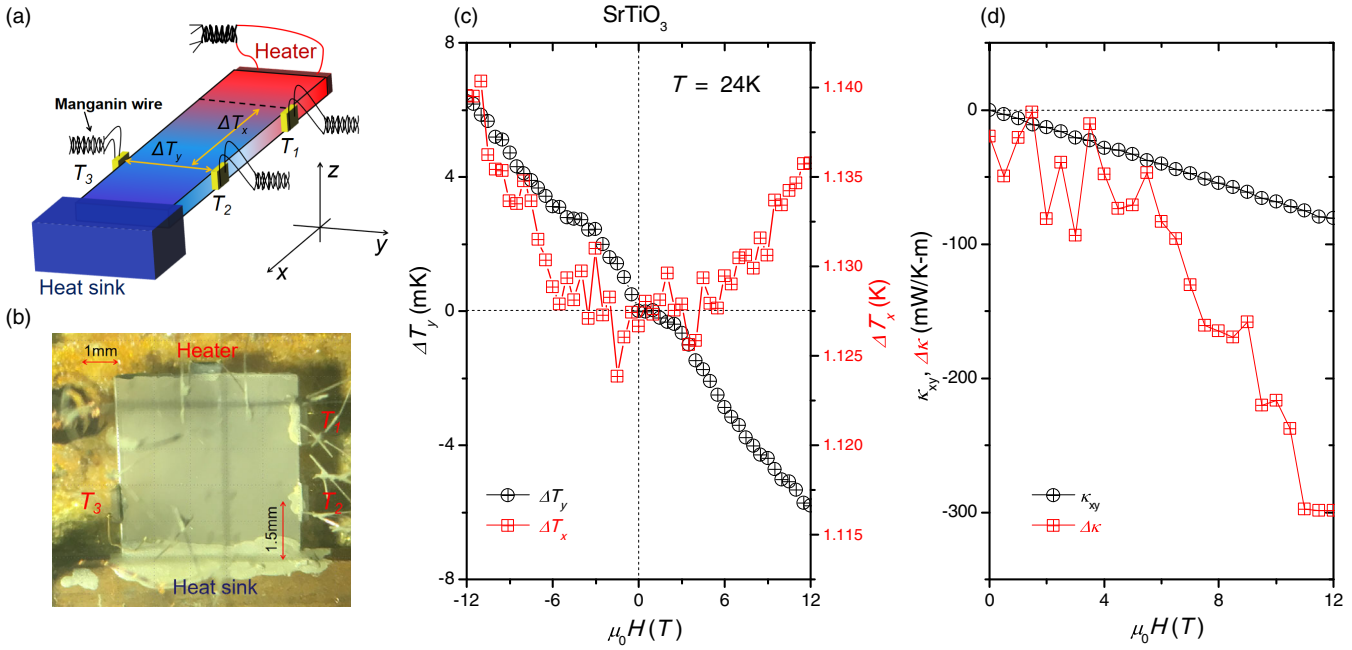

FIG. 1. Quantifying the thermal Hall effect in $SrTiO_3$. (a) Setup for measuring longitudinal and transverse thermal differences ($\Delta T_x = T_1 - T_2$, $\Delta T_y = T_3 - T_2$) generated by a longitudinal thermal current. (b) A photograph of the sample and the setup. The heater and the heat sink were connected to two sides of the sample and at the same level. Three thermometers were mounted near the middle of the sample. (c) Field dependence of ΔT_y and ΔT_x at $T_2 = 24$ K (labeled as sample temperature T below), ΔT_y has been shifted vertically to cancel an unavoidable misalignment offset. Note that ΔT_x is even dominant and ΔT_y is odd dominant in magnetic field. (d) Extracted thermal Hall conductivity κ_{xy} and field-induced change in thermal conductivity $\Delta\kappa = \kappa(\mu_0 H) - \kappa(0)$ as function of field. The latter signal is noisier, because the measurement of ΔT_x has not been done in differential mode.

fluctuations [22]. Upon the introduction of a tiny amount of mobile electrons, this wide-gap insulator turns to a dilute metal [24] subject to a superconducting instability [25,26] and displaying nontrivial charge transport at room temperature [27]. Its cubic crystal structure at room temperature is lost below 105 K [28]. This structural transition is AFD: neighboring TiO_6 octahedra tilt clockwise and anticlockwise. As a consequence, the tiny tetragonal distortion generates significant anisotropy in charge transport [29]. In absence of strain, three possible domains can be present [29]. The polar walls between these micrometric domains have been a subject of numerous studies [30–32].

Previous studies of heat transport in this solid [33–35] uncovered two remarkable features. In a pioneer study, Steigmeier [33] determined the temperature dependence of the thermal conductivity (which peaks to 30 W/K-m at $T \simeq 20$ K), and found that below the maximum, it depends on the applied electric field. More recently, Martelli and coworkers [35] found that thermal conductivity decreases faster than T^3 below the peak. Such a behavior has only been observed in a handful of solids and attributed to the Poiseuille flow of phonons [36], triggered by abundant normal (i.e., momentum-conserving) collisions among phonons. Soft phonons, either those associated with the antiferrodistortive transition [37,38], or modes corresponding to the aborted ferroelectricity [38], are suspected to drive these unusual features of heat transport [35]. This may also be the case of the observation reported in the present Letter.

We measured the thermal Hall effect by using a one-heater-three-thermometers method as shown in Figs. 1(a) and 1(b) (see the Supplemental Material [39] for more details). Figures 1(c)–1(d) shows the data at 24 K. As seen in Fig. 1(c), ΔT_x is an even and ΔT_y is an odd function of magnetic field. ΔT_y, shifted vertically to zero by a tiny quantity due to unavoidable misalignment between T_2 and T_3, has opposite signs for positive and negative magnetic fields, which implies $\kappa_{xy}(\mu_0 H) = -\kappa_{xy}(-\mu_0 H)$, as one would expect for the off-diagonal component of the conductivity tensor. On the other hand, ΔT_x is finite at zero field and increases symmetrically with applied magnetic field implying $\kappa(\mu_0 H) = \kappa(-\mu_0 H)$.

The field dependence of thermal Hall conductivity κ_{xy} and the field-induced change in thermal conductivity $\Delta\kappa = \kappa(\mu_0 H) - \kappa(0)$ at $T = 24$ K are plotted in Fig. 1(d). The magnitude of κ_{xy} attains -80 mW/K-m, twice larger than the maximum observed in cuprates [21]. As seen in the figure, however, this is four times smaller than the field-induced change in longitudinal thermal conductivity, $\Delta\kappa$, itself about one percent of total signal. We note that Jin *et al.* [40] have recently reported on a similar field-induced decrease in the lattice thermal conductivity of another band insulator.

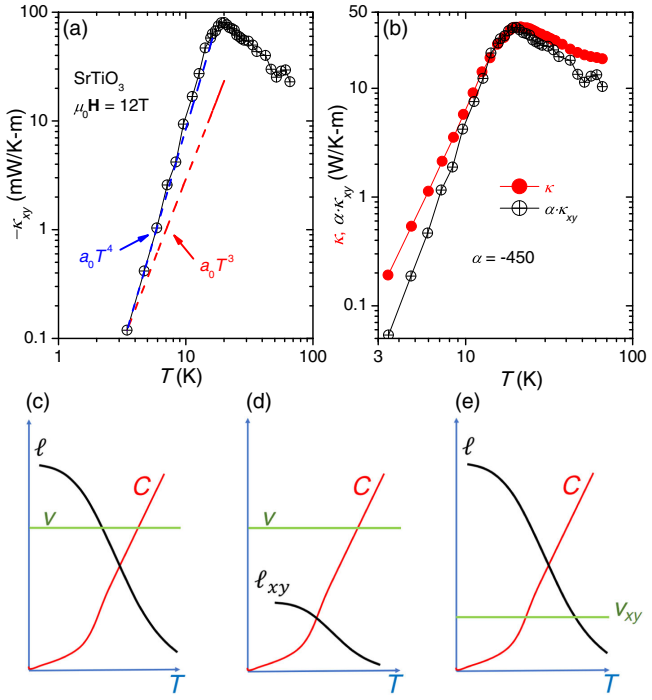

FIG. 2. Thermal Hall conductivity and its correlation with longitudinal thermal conductivity. (a) The temperature dependence of κ_{xy} in presence of a magnetic field of 12 T in $SrTiO_3$. (b) A comparison of the temperature dependence of longitudinal and transverse thermal conductivity, κ_{xy} has been multiplied by a factor α equal to -450. Both peak at the same temperature, but κ_{xy} falls faster at both sides of the peak. (c) Schematic sketch of the temperature dependence of specific heat, mean-free-path and velocity generating a peak in κ. Off-diagonal response may be caused by the skew scattering [transverse mean-free-path ℓ_{xy} (d) or the off-diagonal velocity v_{xy} (e)].

The temperature dependence of κ_{xy} in $SrTiO_3$ is shown in Fig. 2(a). As seen in the figure, in a magnetic field of 12 T, it peaks to -0.08 W/K-m at $\simeq$20 K and falls rapidly at both sides of this peak. Figure 2(b) presents a comparison of the temperature dependence of κ_{xy} and κ, with the former multiplied by a factor $\alpha = -450$. Both peak at the same temperature, but the decrease in κ_{xy} is faster on either sides of the maximum. As found previously [35], κ in $SrTiO_3$ follows T^{β} (with β slightly larger than 3) below the peak temperature. κ_{xy} decreases even more sharply in this regime, and it almost follows a T^4 temperature dependence. With warming, the drop in the transverse signal is slightly sharper than the drop in the longitudinal one.

A phenomenological picture of κ equates it with a product of specific heat, C, velocity, v, and mean-free path, ℓ. This should be summed over different phonon modes, indexed λ:

$$\kappa = \frac{1}{\nu}\sum_{\lambda} C^{\lambda} v^{\lambda} \ell^{\lambda}. \tag{1}$$

Here, ν is a dimension-dependent normalisation factor. Usually, the variation of sound velocity with temperature is negligible. Indeed, the experimentally measured elastic moduli of $SrTiO_3$ [41] (and therefore its sound velocity) changes by less than a few percent in our temperature range of interest. The thermal evolution of the mean-free-path and the specific heat, on the other hand, is strong and opposite to each other [see Fig. 2(c)]. Therefore, in an insulator κ peaks at a temperature where the global phonon trajectory (i.e. phonon population times phonon mean-free path) is maximal. This temperature has a physical significance. Thermal conductivity is most vulnerable to the introduction of point defects near this peak temperature [1]. Our observation that κ_{xy} peaks at this very temperature is a source of information on what causes the transverse signal. Phenomenologically, a finite κ_{xy} implies either an off-diagonal (temperature-independent) velocity or an off-diagonal (temperature-dependent) mean-free path. Therefore:

$$\kappa_{xy} = \frac{1}{\nu}\sum_{\lambda} C^{\lambda}(v^{\lambda}_{xy}\ell^{\lambda} + v^{\lambda}\ell^{\lambda}_{xy}). \tag{2}$$

Presumably, ℓ_{xy} and v_{xy} are both much smaller than their longitudinal counterparts as sketched in Figs. 2(d) and 2(e).

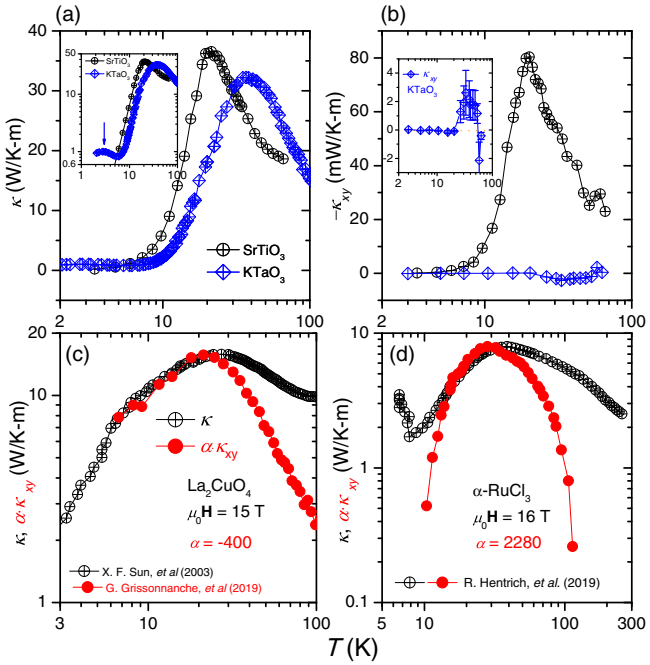

FIG. 3. κ_{xy} and κ in other insulators. (a) Longitudinal thermal conductivity κ in $SrTiO_3$ and $KTaO_3$, the inset shows a logarithmic plot. (b) Transverse thermal conductivity κ_{xy} in $SrTiO_3$ and $KTaO_3$. The inset shows an enlargement of the magnitude of the resolved signal. (c) A comparison of the temperature dependence of κ_{xy} at 15 T (multiplied by -400) with κ [46] in La_2CuO_4. (d) The same comparison in the case of α-$RuCl_3$. Here, κ_{xy} at 16 T is multiplied by 2280. In all these cases, κ_{xy} and κ peak at the same temperature and the transverse signal decreases more rapidly below and above the peak.

Therefore, the fact that κ_{xy} peaks at the same temperature but decreases faster may be ascribed to one of the right-hand terms of Eq. (2) or their combination.

The magnitude of κ_{xy} in strontium titanate is two orders of magnitude larger than what was reported for $Tb_3Ga_3O_{12}$ [4]. This raises a natural question: can proximity to a ferroelectric quantum criticality [42] play a role in generating a large phonon thermal Hall effect? In order to answer this question, we investigated heat transport in $KTaO_3$. This insulator, like $SrTiO_3$, is close to a ferroelectric transition, but its low-temperature electric permittivity is five times smaller [43].

In agreement with what was reported before for $KTaO_3$ [44] and $SrTiO_3$ [33,35], we found that the amplitude of the peak in longitudinal thermal conductivity is comparable (30–35 W/K-m) in the two perovskites [see Fig. 3(a)]. On the other hand, the amplitude of the thermal Hall conductivity is very different. In $KTaO_3$, κ_{xy} is more than one order of magnitude smaller than in $SrTiO_3$ [Fig. 3(b)]. Let us note that even in the case of longitudinal thermal conductivity, there are remarkable differences between these two solids. Around $T \simeq 5$ K, thermal conductivity is sharply decreasing (displaying a faster than cubic temperature dependence) in $SrTiO_3$ but is increasing [presenting an additional bump, as seen in the inset of Fig. 3(a)] in $KTaO_3$. In other words, the consequences of anharmonicity for longitudinal heat transport is qualitatively different in these two apparently similar solids. Structurally, the most notable difference is the absence of the AFD transition in cubic $KTaO_3$ [45], in contrast to its presence in $SrTiO_3$. This is our first evidence that this peculiar structural transition plays a role in setting the amplitude of κ_{xy}.

The correlation between the position of peaks in longitudinal and transverse response in $SrTiO_3$ and $KTaO_3$ led us to put under scrutiny the published data in two other insulators. As seen in Figs. 3(c) and 3(d), according to the available data, there is a similar correlation between $\kappa_{xy}(T)$ and $\kappa(T)$ in both La_2CuO_4 [21,46] and in α-$RuCl_3$ [20]. In all cases, κ_{xy} and κ peak at almost the same temperature and the decrease in κ_{xy} is sharper (or in one case almost equal) to the decrease in κ. We notice that this correlation, which was not reported before, indicates a major role played by the principal heat carriers in setting the transverse response.

Our additional measurements build up the case for a prominent role played by AFD domains. The results are shown in Fig. 4. First of all, we studied three different $SrTiO_3$ samples, provided by two different companies. As shown in Figs. 4(a) and 4(b), all three samples show a sizable κ_{xy}, but different amplitudes. Two samples in which the magnitude of κ is almost the same [Fig. 4(a)], display a threefold difference in their peak of κ_{xy} [Figs. 4(b) and 4(d)]. As seen in Fig. 4(c), the field-induced decrease in κ is roughly the same in the two samples.

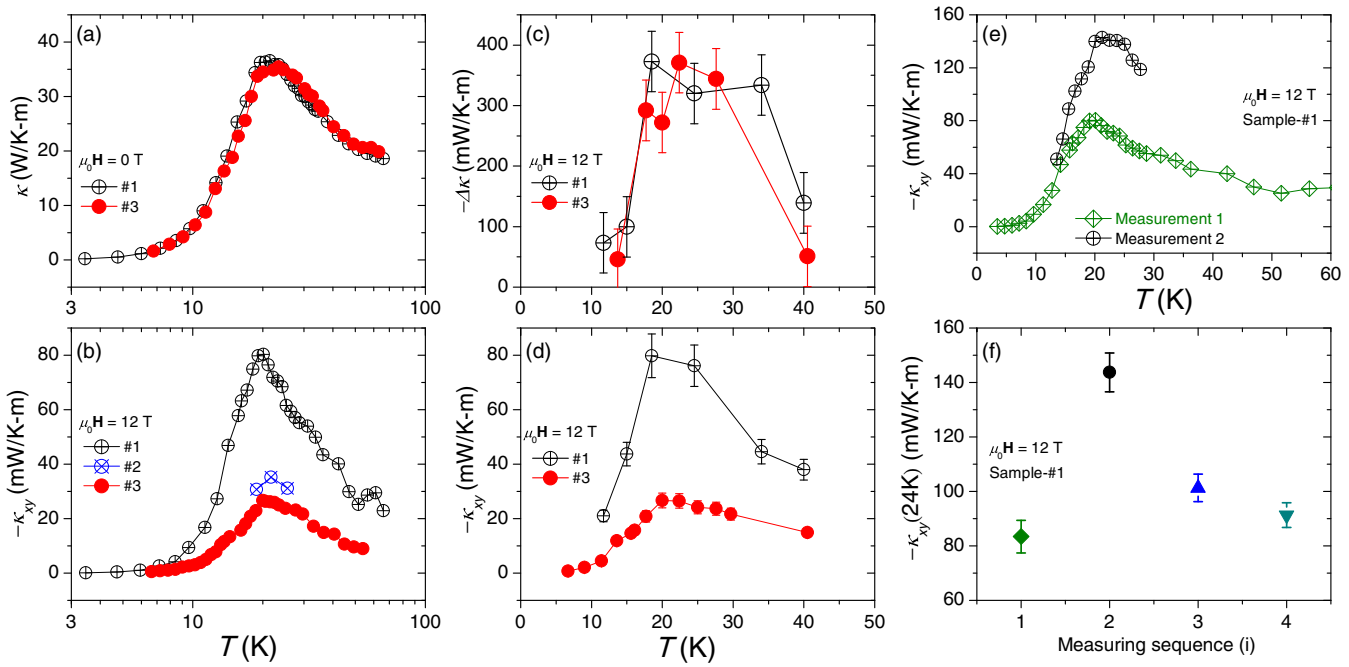

FIG. 4. Variability of κ_{xy} in $SrTiO_3$. (a) $\kappa(T)$ in two different samples, the data is almost same. (b) Temperature dependence of κ_{xy} in three $SrTiO_3$ samples. (c),(d) Two samples with the same field-induced change in κ display a threefold difference in their κ_{xy}, data extracted from the field-sweeping curves. (e) Even in the same sample, the magnitude of κ_{xy} changes after warming it above T_{AFD}. The two curves show the data measured before (measurement 1) and after (measurement 2) being warmed to room temperature and staying in air for days. (f) κ_{xy} of the same sample at 24 K as a function of measuring sequence, separated by the warming history of being warmed to room temperature and staying in air for days, data extracted from the field-sweeping curves.

In a second set of measurements, we repeated our measurements of κ_{xy} on the same sample after warming it above $T_{AFD} = 105$ K and cooling it back again. As seen in Figs. 4(e) and 4(f) (for more details, see the Supplemental Material [39]), warming above the AFD transition temperature can change the magnitude of κ_{xy} ($T = 24$ K) in the same sample.

Buckley *et al.* [30] observed needlelike structural domains below 105 K in $SrTiO_3$ and "found almost no memory of the domain patterns under repeated heating and cooling through the transition point" [30]. The typical size of the observed domains was a micron, comparable to the apparent phonon mean-free-path extracted from longitudinal thermal conductivity and specific heat [35]. An intimate link between domain configuration and the amplitude of κ_{xy} would explain why the amplitude of κ_{xy} can be different after thermal cycling above T_{AFD}, wiping out the previous configuration of domains. Obviously, the sample dependence of the signal and its virtual absence in $KTaO_3$ also find natural explanations.

Theoretical scenarios for phonon thermal Hall effect [5–11] either invoke skew scattering of heat carriers or let the magnetic field generate a transverse velocity. Let us have a look to our results in either of these schemes. One may be tempted to attribute the observed κ_{xy} to skew scattering of phonons by the AFD domain walls, which according to a number of experiments [31,32] are polar. However, the skew-scattering picture would have a hard time to explain the disconnection between the field-induced decrease in κ and the finite κ_{xy} [Figs. 4(c) and 4(d)]. Alternatively, one may point to the fact that the slight tetragonal distortion leads to quasidegenerate acoustic phonon modes and it has been suggested [47] that the acoustic phonons hybridize with the transverse optical phonons. Thanks to these features, the magnetic field may become able to couple to titanium-oxygen ionic bonds [11] and generate a transverse velocity. Presumably, this should crucially depend on the relative orientation of the magnetic field and each of the three tetragonal domains; hence a dependence on precise domain configuration. Note that *ab initio* theoretical calculations find imaginary frequencies [48] for strontium titanate. Two recent theoretical studies succeeded in finding real phonon frequencies [49,50]. However, the focus of both was the cubic state and the phonon spectrum below the AFD transition remains unknown. Future theoretical studies may fill this void. Future experiments may use strain to control the configuration of domains.

In summary, phonons in $SrTiO_3$ can generate a κ_{xy} larger than what was reported in any other insulator. This is not generic to all quantum paraelectric solids and appear to be intimately linked to the occurrence of an AFD transition in $SrTiO_3$. We find that not only in $SrTiO_3$, but also in other insulators κ_{xy} and κ peak at the same temperature. The observation appears as a clue to identify carriers and collisions which generate the transverse signal. In the case of $SrTiO_3$, two experimental observations point to the role of tetragonal domains in generating the signal.

We are grateful to Jing-yuan Chen, Gaël Grissonnanche, Steve Kivelson, and Louis Taillefer for stimulating discussions. This work was supported by the Agence Nationale de la Recherche (ANR-18-CE92-0020-01). B. F. acknowledges support from Jeunes Equipes de l'Institut de Physique du Collge de France (JEIP). Z. Z. acknowledges support from the National Science Foundation of China (Grants No. 11574097 and No. 51861135104) and The National Key Research and Development Program of China (Grant No. 2016YFA0401704). X. L. acknowledges a PhD scholarship by the China Scholarship Council (CSC).

[1] R. Berman, *Thermal Conduction in Solids* (Oxford University Press, Oxford, 1976).
[2] L. Lindsay, A. Katre, A. Cepellotti, and N. Mingo, J. Appl. Phys. **126**, 050902 (2019).
[3] C. Strohm, G. L. J. A. Rikken, and P. Wyder, Phys. Rev. Lett. **95**, 155901 (2005).
[4] A. V. Inyushkin and A. N. Taldenkov, JETP Lett. **86**, 379 (2007).
[5] L. Sheng, D. N. Sheng, and C. S. Ting, Phys. Rev. Lett. **96**, 155901 (2006).
[6] Yu. Kagan and L. A. Maksimov, Phys. Rev. Lett. **100**, 145902 (2008).
[7] J.-S. Wang and L. Zhang, Phys. Rev. B **80**, 012301 (2009).
[8] L. Zhang, J. Ren, J.-S. Wang, and B. Li, Phys. Rev. Lett. **105**, 225901 (2010).
[9] T. Qin, J. Zhou, and J. Shi, Phys. Rev. B **86**, 104305 (2012).
[10] M. Mori, A. Spencer-Smith, O. P. Sushkov, and S. Maekawa, Phys. Rev. Lett. **113**, 265901 (2014).
[11] B. K. Agarwalla, L. Zhang, J.-S. Wang, and B. Li, Eur. Phys. J. B **81**, 197 (2011).
[12] Y. Onose, T. Ideue, H. Katsura, Y. Shiomi, N. Nagaosa, and Y. Tokura, Science **329**, 297 (2010).
[13] J. Liu, L. J. Cornelissen, J. Shan, T. Kuschel, and B. J. van Wees, Phys. Rev. B **95**, 140402(R) (2017).
[14] S. Murakami and A. Okamoto, J. Phys. Soc. Jpn. **86**, 011010 (2017).
[15] M. Hirschberger, J. W. Krizan, R. J. Cava, and N. P. Ong, Science **348**, 106 (2015).
[16] K. Sugii, M. Shimozawa, D. Watanabe, Y. Suzuki, M. Halim, M. Kimata, Y. Matsumoto, S. Nakatsuji, and M. Yamashita, Phys. Rev. Lett. **118**, 145902 (2017).
[17] T. Ideue, T. Kurumaji, S. Ishiwata, and Y. Tokura, Nat. Mater. **16**, 797 (2017).
[18] Y. Kasahara, K. Sugii, T. Ohnishi, M. Shimozawa, M. Yamashita, N. Kurita, H. Tanaka, J. Nasu, Y. Motome, T. Shibauchi, and Y. Matsuda, Phys. Rev. Lett. **120**, 217205 (2018).
[19] Y. Kasahara, T. Ohnishi, Y. Mizukami, O. Tanaka, S. Ma, K. Sugii, N. Kurita, H. Tanaka, J. Nasu, Y. Motome, T. Shibauchi, and Y. Matsuda, Nature (London) **559**, 227 (2018).
[20] R. Hentrich, M. Roslova, A. Isaeva, T. Doert, W. Brenig, B. Büchner, and C. Hess, Phys. Rev. B **99**, 085136 (2019).

[21] G. Grissonnanche, A. Legros, S. Badoux, E. Lefrançois, V. Zatko, M. Lizaire, F. Laliberté, A. Gourgout, J.-S. Zhou, S. Pyon, T. Takayama, H. Takagi, S. Ono, N. Doiron-Leyraud, and L. Taillefer, Nature (London) **571**, 376 (2019).
[22] K. A. Müller and H. Burkard, Phys. Rev. B **19**, 3593 (1979).
[23] C. Collignon, X. Lin, C. W. Rischau, B. Fauqueé, and K. Behnia, Annu. Rev. Condens. Matter Phys. **10**, 25 (2019).
[24] A. Spinelli, M. A. Torija, C. Liu, C. Jan, and C. Leighton, Phys. Rev. B **81**, 155110 (2010).
[25] J. F. Schooley, W. R. Hosler, and M. L. Cohen, Phys. Rev. Lett. **12**, 474 (1964).
[26] X. Lin, Z. Zhu, B. Fauqueé, and K. Behnia, Phys. Rev. X **3**, 021002 (2013).
[27] X. Lin, C. W. Rischau, L. Buchauer, A. Jaoui, B. Fauqueé, and K. Behnia, npj Quantum Mater. **2**, 41 (2017).
[28] G. Shirane and Y. Yamada, Phys. Rev. **177**, 858 (1969).
[29] Q. Tao, B. Loret, B. Xu, X. Yang, C. W. Rischau, X. Lin, B. Fauqueé, M. J. Verstraete, and K. Behnia, Phys. Rev. B **94**, 035111 (2016).
[30] A. Buckley, J. P. Rivera, and E. K. H. Salje, J. Appl. Phys. **86**, 1653 (1999).
[31] J. F. Scott, E. K. H. Salje, and M. A. Carpenter, Phys. Rev. Lett. **109**, 187601 (2012).
[32] E. K. H. Salje, O. Aktas, M. A. Carpenter, V. V. Laguta, and J. F. Scott, Phys. Rev. Lett. **111**, 247603 (2013).
[33] E. F. Steigmeier, Phys. Rev. **168**, 523 (1968).
[34] X. Lin, A. Gourgout, G. Bridoux, F. Jomard, A. Pourret, B. Fauqué, D. Aoki, and K. Behnia, Phys. Rev. B **90**, 140508(R) (2014).
[35] V. Martelli, J. L. Jiménez, M. Continentino, E. Baggio-Saitovitch, and K. Behnia, Phys. Rev. Lett. **120**, 125901 (2018).
[36] H. Beck, P. F. Meier, and A. Thellung, Phys. Status Solidi (A) **24**, 11 (1974).
[37] Y. Yamada and G. Shirane, J. Phys. Soc. Jpn. **26**, 396 (1969).
[38] H. Vogt, Phys. Rev. B **51**, 8046 (1995).
[39] See the Supplemental Material at http://link.aps.org/supplemental/10.1103/PhysRevLett.124.105901 for more information on samples, the measurement techniques, and a few additional results.
[40] H. Jin, O. D. Restrepo, N. Antolin, S. R. Boona, W. Windl, R. C. Myers, and J. P. Heremans, Nat. Mater. **14**, 601 (2015).
[41] W. Rehwald, Solid State Commun. **8**, 1483 (1970).
[42] S. E. Rowley, L. J. Spalek, R. P. Smith, M. P. M. Dean, M. Itoh, J. F. Scott, G. G. Lonzarich, and S. S. Saxena, Nat. Phys. **10**, 367 (2014).
[43] R. P. Lowndes and A. Rastogi, J. Phys. C **6**, 932 (1973).
[44] M. Tachibana, T. Kolodiazhnyi, and E. Takayama-Muromachi, Appl. Phys. Lett. **93**, 092902 (2008).
[45] H. H. Barrett, Phys. Lett. **26A**, 217 (1968).
[46] X. F. Sun, J. Takeya, S. Komiya, and Y. Ando, Phys. Rev. B **67**, 104503 (2003).
[47] A. Bussmann-Holder, Phys. Rev. B **56**, 10762 (1997).
[48] U. Aschauer and N. A. Spaldin, J. Phys. Condens. Matter **26**, 122203 (2014).
[49] L. Feng, T. Shiga, and J. Shiomi, Appl. Phys. Express **8**, 071501 (2015).
[50] T. Tadano and S. Tsuneyuki, Phys. Rev. B **92**, 054301 (2015).